Molecular Dynamics Simulation Study of Isotropic and Nematic PCH-5

G. Krömer, D. Paschek, and A. Geiger

Physikalische Chemie, Universität Dortmund, D-44221 Dortmund

Key Words: Computer Experiments / Diffusion / Liquid Crystals / Molecular Interactions / Statistical Mechanics

4-(trans-4-Pentyl-cyclohexyl)-benzonitril (PCH-5) has been studied by molecular dynamics simulations of the isotropic liquid as well as the nematic mesophase. The intra- and intermolecular interaction are described in pseudoatom approach. Besides the nematic order parameters S we calculate various distributions functions to characterize and compare the microscopic structure. In both phases we find a distinct antiparallel arrangement of neighbouring molecules, in accord with the known crystal structure of homologous substances. The molecular dynamics shows strong anisotropic behaviour in both phases. The corresponding diffusion coefficients are determined and compared with an experimental value.

1. Introduction

Computer simulations of liquid crystals are performed on different levels of model refinement. Systems of hard ellipsoids of revolution give valuable insight into general mechanisms of phase transitions, for example by establishing the minimum molecular anisotropy required for the appearance of the liquid crystalline phase [1]. To get closer contact to real liquid crystalline compounds and to be in a position to reproduce and study the influence of chemical modifications, a much more specific description of intra- and intermolecular interactions has to be used.

At present, such simulations, which are based on detailed atom-atom potentials for actual molecules and very demanding in computer time, are restricted to single state points. Nevertheless, a few such studies have been reported until now [2–4]. In this paper first results from molecular dynamics simulations of a realistic model of 4-(trans-4-pentylcyclohexyl)benzonitril (PCH-5) are given. We allow for intramolecular flexibility and chemically specific intramolecular interaction through the use of a standard molecular mechanics force field [5]. The isotropic and nematic phases of this model liquid are simulated. The goals of this ongoing study are to establish the ability of such simulations to reproduce the properties of the real substance (essentially this is determined by the quality of the force field), to gain a detailed picture of the microscopic structure and dynamics and to study the influence of prominent features of the interaction model (like the polarity of the cyano group) on such properties.

2. Simulations

In molecular dynamics simulations Newton's equations of motion for a system of N interacting particles are numerically integrated. The potential energy U of the system is expressed in terms of an analytic function. An accepted approach is given by the representation of U as a function of the internal degrees of freedom and interatomic distances as it is implemented in the GROMOS [5] code:

$$U = \sum_b \frac{1}{2} k_b (b - b_0)^2 + \sum_\theta \frac{1}{2} k_\theta (\theta - \theta_0)^2 + \sum_\xi \frac{1}{2} k_\xi (\xi - \xi_0)^2 + \sum_\phi k_\phi (1 + \cos(n\phi - \delta)) + \sum_{i<j} \left[\left(\frac{A_{ij}}{r_{ij}^{12}} - \frac{B_{ij}}{r_{ij}^{6}} \right) + \left(\frac{q_i q_j}{4\pi\varepsilon_0 r_{ij}} \right) \right]$$

where $k_b, k_\theta, k_\xi, k_\phi$ are force constants representing bond stretching, bond bending, improper torsion and torsion motion respectively. The distance between the interacting sites i and j is r_{ij}, A_{ij}, B_{ij} and q are the parameters for the Lennard-Jones and electrostatic terms. The force field parameters used in this study are listed in Tables 3 to 7.

We employ the united atom approximation, i.e., hydrogen atoms are included in the parameters of the carbon atoms (Fig. 1). These parameters are not appropriate to describe the intramolecular 1–4 interactions correctly. Therefore in these cases reduced parameters, as given in Table 7, are used [2, 5].

The SHAKE algorithm is used to eliminate the bond stretching motions to keep the bond distances constant; this allows integration timesteps of 2 fs. Molecular dynamics simulations were performed for systems of 50 and 100 PCH-5 molecules using rectangular periodic boundary conditions. The interactions are calculated with the minimum image convention applying a cut-off radius of 1 nm. The

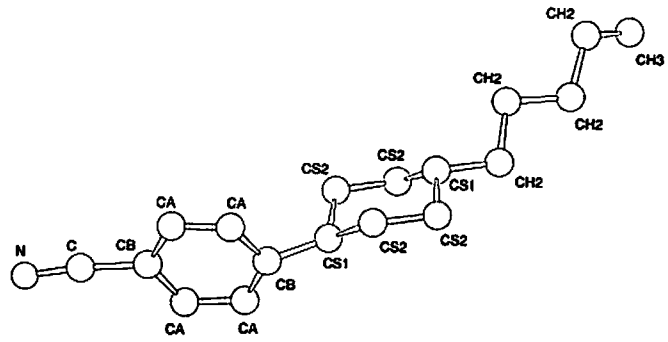

Fig. 1
United atom model of 4-(trans-4-pentylcyclohexyl)benzonitril. The assignment of atom types as used in Tables 3 to 7 is shown

  0005-9021/93/1010-1188 $ 10.00+.25/0

isotropic and the nematic phases were simulated at the same constant temperature (333 K) and constant pressure (1 atm).

The chosen temperature is close to the clearing point of the real substance ($T_C = 328$ K). This value is not known for our model substances. In consequence, one of the two simulated phases must be metastable, although no indication for a drift versus a phase transition could be observed in either simulation. The identity of the temperatures for both phases allows a comparison of structure and dynamics, excluding temperature effects.

Partial charges were put on the cyano group only and varied in the following way. In one set of simulations parameters of the GROMOS-Potential ($q = \pm 0.28\,e$) were used. This results in a dipole moment, which is too low in comparison with the experimental value. Applying higher charges ($q = \pm 0.5\,e$), as delivered by the CHARMM [6, 7]

Table 1
Translational diffusion coefficients

Simulation No.	phase	number of molecules	partial charges on cyano groups	D_t / $10^{-10}\,m^2\,s^{-1}$	$D_\parallel$ / $10^{-10}\,m^2\,s^{-1}$	$D_\perp$ / $10^{-10}\,m^2\,s^{-1}$	$D_\parallel / D_\perp$
1	isotropic	50	0.28e	1.10	1.94	0.68	2.9
2	isotropic	50	0.50e	0.76	1.49	0.40	3.7
3	nematic	50	0.50e	0.40	0.65	0.27	2.4
4	nematic	100	0.50e	0.31	0.56	0.18	3.1
5	nematic	100	0.28e	0.83	1.57	0.46	3.4

$D_{exp} = 1.0 \cdot 10^{-10}\,m^2\,s^{-1}$ [13]

Table 2
Order parameters and rotational diffusion coefficients

Simulation No.	S	$D_\parallel^{rot}$ / $10^{-9}\,s^{-1}$	$D_\perp^{rot}$ / $10^{-8}\,s^{-1}$	$D_\parallel^{rot} / D_\perp^{rot}$
1	0.14	3.1	2.2	14
2	0.17	3.3	1.8	18
3	0.61	1.3	0.6	22
4	0.61	1.5	0.5	30
5	0.58	3.8	1.6	24

Table 3
Bond stretching parameters

Bond	k_b/kcal mol^{-1} Å^{-2}	b_0/Å
N–C	1000.0	1.33
C–CB	800.0	1.53
CB–CA	1000.0	1.39
CA–CA	1000.0	1.39
CB–CS1	800.0	1.53
CS1–CS2	600.0	1.53
CS2–CS2	800.0	1.53
CS1–CH2	800.0	1.53
CH2–CH2	800.0	1.53
CH2–CH3	800.0	1.53

Table 4
Bond bending parameters

Angle	k_ϑ/kcal mol^{-1} rad^{-2}	ϑ_0/°
N–C–CB	120.0	180.0
C–CB–CA	100.0	120.0
CB–CA–CA	100.0	120.0
CB–CS1–CS2	60.0	109.5
CS1–CS2–CS3	60.0	109.5
CS1–CH2–CH2	110.0	111.0
CH2–CH2–CH2	110.0	111.0
CH2–CH2–CH3	110.0	111.0

Table 5
Improper torsional parameters

Torsion	k_ζ/kcal mol^{-1} rad^{-2}	ζ_0/°
X–CA–CA–Y	40.0	0.0
X–CA–CB–Y	40.0	0.0
X–C–CA–Y	40.0	0.0

Table 6
Torsional parameters

Torsion	k_φ/kcal mol^{-1}	n	δ
X–CB–CS1–Y	1.4	3	0
X–CS1–CS2–Y	1.4	3	0
X–CS2–CS2–Y	1.4	3	0
X–CS1–CH2–Y	1.4	3	0
X–CH2–CH2–Y	1.4	3	0

Table 7
Lennard-Jones parameters for interactions between atoms of the same type. For interactions between atoms of different type combination rules are used [2, 5]. Reduced values for intramolecular (1–4) interactions are marked accordingly

Atom	$A_{ij}/10^6$ kcal mol^{-1} Å^{12}	$B_{ij}/10^3$ kcal mol^{-1} Å^6
N	0.404	0.582
C	0.806	0.559
CB	0.806	0.559
CA	3.614	1.318
CA (1–4)	1.991	1.321
CS1	17.148	2.987
CS1 (1–4)	0.893	0.696
CS2	8.445	2.174
CS2 (1–4)	1.700	1.128
CH2	8.445	2.174
CH2 (1–4)	1.700	1.129
CH3	6.250	2.122
CH3 (1–4)	2.883	1.638

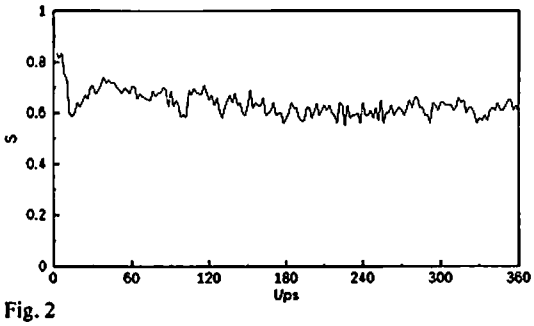

Fig. 2
Temporal development of the order parameter during 120 ps relaxation and 240 ps sampling period (simulation 3)

force field, yields a dipole moment comparable with the experimental value, but it should be noted, that this moment is strongly localized.

The isotropic phase was obtained by heating an ordered starting configuration to 1000 K and subsequently cooling it down. After sufficient equilibration of 100 ps the simulation time was 240 ps.

The nematic system was produced from the isotropic liquid by applying an external potential

$$V = k(1 - \cos^2 \theta)$$

where $k = 100$ kJ/mol and θ stands for the angle between the CN bond and the z-axis of the box. Afterwards the system was allowed to relax without the extra potential for 120 ps, before the proper sampling period of 240 ps started. Fig. 2 gives the temporal development of the order parameter during relaxation and sampling period. In Fig. 3 a snapshot of the obtained nematic structure is shown for illustration.

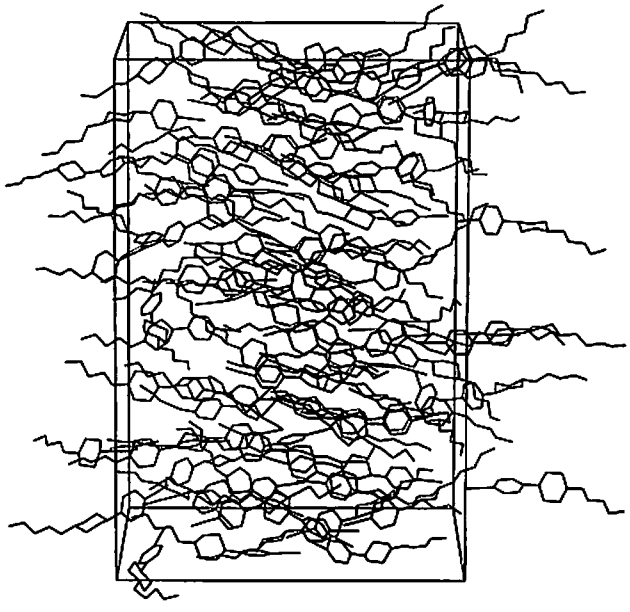

Fig. 3
Snapshot of the nematic phase (simulation 4)

3. Results and Discussion

3.1 Structural Properties

We follow Eppenga and Frenkel [8] in calculating the order parameter $S = \langle P_2(\cos\theta)\rangle$ as minus twice the middle eigenvalue of the time averaged ordering tensor whose components are

$$Q_{\alpha\beta} = \frac{1}{N}\sum_i (3u_{i\alpha}u_{i\beta} - \delta_{\alpha\beta})/2$$

where u_i is the unit vector along the CN-bond for each molecule i. The order parameters for the nematic phases as given in Table 2 lie between the experimental values of Yakovenko [9] and Abdoh et al. [10] near the phase transition temperature. For the isotropic phases the simulated values of S are not zero, because of the finiteness of the system, but much below any value given for the nematic phase of PCH-5. This is in accord with the results of simulations of CCH5 [3] and 6OCB [4].

The local structure of the isotropic and the nematic phases can be described by radial distribution and orientational correlation functions. Figs. 4 and 5 show atom-atom radial distribution functions of the isotropic phase for the carbon positions of the cyano head groups as well as for the methyl endgroups. Fig. 4 indicates a strong correlation between the polar and rigid head groups and a much more smeared out distribution of the flexible tails. As one can see from Fig. 5 an increased dipole moment increases appreciably the correlation between the cyano group positions.

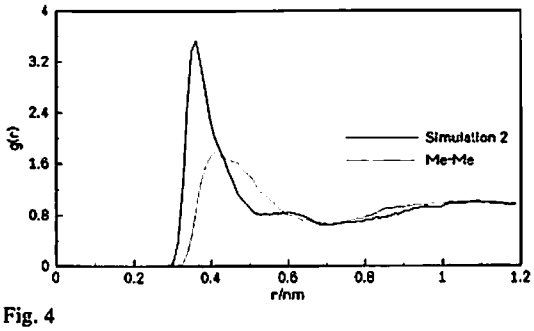

Fig. 4
Carbon-carbon pair distribution functions for the cyano- and the methyl groups (simulation 2)

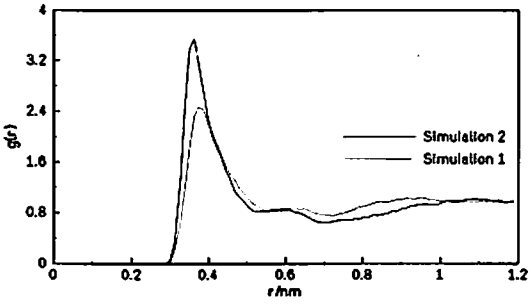

Fig. 5
Carbon-carbon pair distribution functions for the cyano group from simulation runs with different partial charges

To get a more detailed picture of the local structure, we also calculate orientational correlation functions, i.e., normalized expansion coefficients of the orientation-dependent pair correlation function. We consider the easily interpretable functions

$$P_{uu}(r) = \langle \cos \phi_{ij} \rangle_r = \langle u_i u_j \rangle_r$$

$$P_{ue}(r) = \langle \cos \theta_{ij} \rangle_r = \langle e_{ij} u_i \rangle_r$$

Here u_i is an intramolecular unit vector in molecule i, either the C–N vector for the head group or the methylen-methyl vector for the tail. e_{ij} is the intermolecular unit vector pointing from the cyano carbons of molecules j to i. Fig. 6 compares the mutual orientation of cyano groups with the mutual orientation of the final C–C vectors. The strong antiparallel orientation of neighbouring cyano-groups leads to the minimum of $P_{uu}(r)$ at the distance of about 3.5 Å, where the maximum of the radial distribution function was found (Fig. 5). Comparable to Fig. 4, the flexibility of the tail leads to a very weak intermolecular orientational correlation between the final C–C bonds.

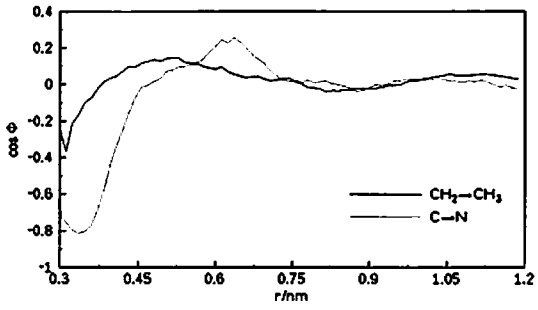

Fig. 6
Orientational correlation functions $P_{uu}(r)$, describing the mutual orientation between the C–N and CH_2-CH_3-vectors (simulation 2)

In Fig. 7 the above discussed mutual orientation of the cyano group is compared for different head group polarities as well as for different phases. What can be seen easily is a more pronounced antiparallel alignment of neighbours with increasing dipole moment and when passing from the isotropic to the nematic phase. Using point charges of $\pm 0.5\,e$ for the cyano groups leads to a nearly perfect antiparallel alignment, with $\langle \cos \phi_{ij} \rangle$ very close to -1. It is also quite interesting to see that antiparallel orientation, as it is well known from the crystal structure of the homologous substance PCH-8 [11], is not only found in the nematic, but slightly less pronounced also in the isotropic phase.

The arrangement of neighbouring pairs in the crystal structure can be described by a partial 'overlapping' of antiparallel molecules. A similar preferential arrangement can be found in the nematic phase, as indicated by the rather positive values of $P_{ue}(r)$ at nearest neighbour distances (see Fig. 8). To summarize, Fig. 9 shows a pair of molecules arbitrary picked from a simulation, which illustrates the above discussion.

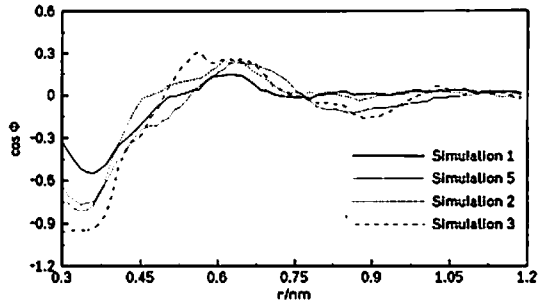

Fig. 7
Orientational correlation functions $P_{uu}(r)$, describing the mutual orientation between the cyano groups for simulation runs with different partial charges and for different phases (see text)

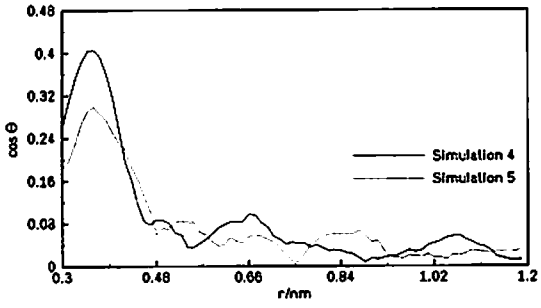

Fig. 8
Orientational correlation functions $P_{ue}(r)$, describing the C–N-vector orientation relative to the connection line between CN and CN

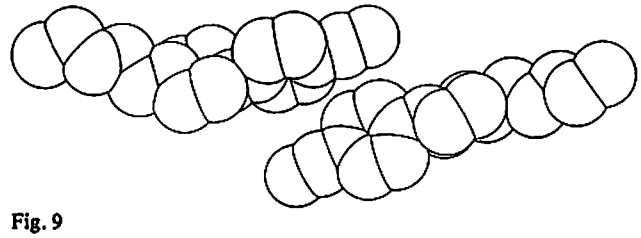

Fig. 9
Arbitrarily chosen molecular pair, illustrating the preferential arrangement of neighbours

3.2 Dynamical Properties

3.2.1 Translational Diffusion

In anisotropic systems such as liquid crystals an anisotropy of the diffusive motion is usually observed. In particular, the self diffusion coefficient along the symmetry axis of the molecule, $D_{\parallel}$, is greater than that perpendicular to the axes, $D_{\perp}$ [12]. We calculated self diffusion coefficients from the mean-square displacements of the center of mass. The obtained values are given in Table 1 and have to be assigned with statistical error bars between 10 and 20%. Within these error bars, we obtain good agreement of the mean value $D_t = (D_{\parallel} + 2D_{\perp})/3$ with a recently determined experimental value for the isotropic liquid at the same temperature [13], the lower partial charges of simulation 1 appearing to be more appropriate. It is quite interesting to see that within the larger error bars of the anisotropy $D_{\parallel}/D_{\perp}$, this value is roughly the same for both phases and both sets

of partial charges. Of course, concerning the isotropic phase, this is only true for short times of the order of the simulation run. For much larger times the isotropy of the system will finally lead to an isotropic displacement.

In contrast to the less effected anisotropy ratio, the absolute values of $D_{\parallel}$ and $D_{\perp}$ systematically decrease with increasing partial charges of the head group. A closer inspection of Table 1 also reveals that single particle dynamics is not strongly influenced by the chosen system size (this is obviously even true for the order parameter S given in Table 2).

Chu and Mori [14] derived an expression relating the anisotropy ratio with the order parameter S and the shape anisotropy of the molecules

$$\gamma = \frac{\pi d}{4l}$$

(with d the diameter and l the length of the rod-like molecules):

$$\frac{D_{\parallel}}{D_{\perp}} = \frac{2\gamma(1-S)+2S+1}{\gamma(S+2)+1-S} .$$

Using $S \approx 0.6$ from Table 1 and $D_{\parallel}/D_{\perp} \approx 3.0$, a shape anisotropy $l/d \approx 5$ is obtained. This value is larger than one would expect from a single PCH-5 molecule, but seems to be more appropriate for 'dimers' as depicted in Fig. 9. This may be interpreted as a hint that pair geometries, as discussed in the previous section, strongly influence the translational diffusive behaviour.

3.2.2 Rotational Diffusion

To describe the rotational motion of the PCH-5 molecules, we make the assumption that the molecules are symmetric-top diffusors, symmetric with respect to their long axis. Then we have to determine the rotational diffusion coefficients $D_{\perp}^{\mathrm{rot}}$, which characterizes the reorientation of the symmetry axis (tumbling motion) and $D_{\parallel}^{\mathrm{rot}}$, describing the rotation around the axis of symmetry (spinning motion). These diffusion coefficients were determined by first calculating from the simulation run time correlation functions

$$C_m^l(t) = \langle D_{mm}^l(\delta\Omega(t)) \rangle$$

where $D_{mk}^l(\delta\Omega)$ are the Wigner rotation matrix elements and the angle of rotation relates to the rigid benzyl-unit of the molecule. The calculation of $\langle D_{mm}^l(\delta\Omega(t)) \rangle$ follows the scheme of Lynden-Bell and Stone [15]. The rotational diffusion coefficients are then determined by fitting the reorientation correlation functions to the Debye-Model

$$C_m^l(t) = \exp\left[(-l(l+1)D_{\perp} - m^2(D_{\parallel} - D_{\perp}))t\right] .$$

The $m = 0$ functions from the simulation scale perfectly with l, whereas for $m \neq 0$ slightly different values for $D_{\parallel}^{\mathrm{rot}}$ are obtained (not shown here). This indicates that the reorientation of the long axis closely resembles a microstep diffusion process, whereas the spinning motion deviates from this model, resulting in larger error bars of about 30% for $D_{\parallel}^{\mathrm{rot}}$. The results given in Table 2 show a strong anisotropy which increases in the nematic phase.

4. Conclusions

In this contribution we discuss a few properties as obtained from an extensive simulation study of the substance PCH-5. We give a detailed description of the microscopic structure and the anisotropic single particle diffusion behaviour. Comparison with experimental results shows that our simulations are quite realistic. However, there is a demand for further improvement. For example, some more recent data evaluation, where we compare the internal flexibility of the simulated molecules with nuclear magnetic relaxation data, reveals that these molecules are too rigid (this will be discussed in more detail elsewhere). We also believe that the Coulomb interaction part of the employed force field should be improved by careful determination of the partial charges. In sum, simulations of this type can provide realistic models to support the interpretation of experimental data as well as to provide useful information on the relations between the properties of single molecules and macroscopic many particle systems.

Financial support from Deutsche Forschungsgemeinschaft and E. Merck Company, Darmstadt is gratefully acknowledged. We also thank HLRZ Jülich for a generous amount of computer time.

References

[1] D. Frenkel in 'Phase Transitions in Liquid Crystals', ed. by S. Martellucci and A.N. Chester, Plenum Press 1992.
[2] S.J. Picken, W.F. van Gunsteren, P.T.H. van Duijnen, and W.H. de Jeu, Liq. Cryst. *6*, 357 (1989).
[3] M.R. Wilson and M.P. Allen, Mol. Cryst. Liq. Cryst. *198*, 465 (1991); M.R. Wilson and M.P. Allen, Liq. Cryst. *12* (1), 157 (1992).
[4] I. Ono and S. Kondo, Bull. Chem. Soc. Jpn. *66*, 633 (1993).
[5] GROMOS (Groningen Molecular Simulation) is a software package developed by W.F. van Gunsteren and H.J.C. Berendsen, University of Groningen 1987.
[6] B.R. Brooks, R.E. Bruccoleri, B.D. Olafson, D.J. States, S. Swaminathan, and M. Karplus, J. Comput. Chem. *4*, 187 (1983).
[7] L. Nilsson and M. Karplus, J. Comput. Chem. *7*, 591 (1986).
[8] R. Eppenga and D. Frenkel, Mol. Phys. *52*, 1303 (1984).
[9] S.Ye. Yakovenko, G. Krömer, and A. Geiger, submitted to Liq. Cryst.
[10] M.M.M. Abdoh et al., J. Chem. Phys. *77*, 2570 (1982).
[11] H. Paulus and W. Haase, Mol. Cryst. Liq. Cryst. *92*, 237 (1983).
[12] G.J. Krueger, Phys. Rep. *82*, 229 (1982).
[13] M. Holz, private communication.
[14] J.K.-S. Chu and D.S. Mori, J. Phys. Colloq. *36*, 1 (1975).
[15] R.M. Lynden-Bell and A.J. Stone, Molec. Simul. *3*, 271 (1989).

Presented at the 92nd Annual Meeting of the Deutsche Bunsen-Gesellschaft für Physikalische Chemie "Neue Eigenschaften und Anwendungen von Flüssigkristallen" in Leipzig, from May 20th to May 22nd, 1993 E 8421